OPEN

Evaluation of LAT1 Expression in Patients With Lung Cancer and Mediastinal Tumors

^{18}F-FBPA PET Study With Immunohistological Comparison

Tadashi Watabe, MD, PhD,† Naoko Ose, MD,‡ Sadahiro Naka, MS,§ Eriko Fukui, MD, PhD,‡ Toru Kimura, MD, PhD,‡ Takashi Kanou, MD, PhD,‡ Soichiro Funaki, MD, PhD,‡ Hidetaka Sasaki, BS,|| Takashi Kamiya, PhD,|| Kenta Kurimoto, BS,§ Kayako Isohashi, MD, PhD,*† Mitsuaki Tatsumi, MD, PhD,†|| Eku Shimosegawa, MD, PhD,†¶ Hiroki Kato, MD, PhD,*† Ryuichi Ohgaki, PhD,** Yoshikatsu Kanai, MD, PhD,** and Yasushi Shintani, MD, PhD‡*

Purpose of the Report: L-type amino acid transporter-1 (LAT1) is a tumor-specific transporter expressed in various tumor types, with minimal expression in normal organs. We previously demonstrated ^{18}F-fluoro-borono-phenylalanine (^{18}F-FBPA) as a selective PET probe for LAT1 in a preclinical study. Herein, we evaluated LAT1 expression in preoperative patients with lung or mediastinal tumors using ^{18}F-FBPA PET and immunofluorescence staining.

Patients and Methods: The study population included patients with histopathological diagnosis (n = 55): primary lung cancers (n = 21), lung metastases (n = 6), mediastinal tumors (n = 15), and benign lesion (n = 13). PET scanning was performed 1 hour after the injection of ^{18}F-FBPA (232 ± 32 MBq). Immunofluorescence staining was performed on the resected tumor sections using LAT1 antibody. LAT1 staining was graded on a 4-grade scale and compared with the SUV_{max} on ^{18}F-FBPA PET.

Results: A positive correlation was observed between the SUV_{max} of ^{18}F-FBPA PET and LAT1 expression by immunofluorescence staining ($r = 0.611$, $P < 0.001$). The SUV_{max} of ^{18}F-FBPA was 3.92 ± 1.46 in grade 3, 3.21 ± 1.82 in grade 2, 2.33 ± 0.93 in grade 1, and 1.50 ± 0.39 in grade 0 of LAT1 expression. Although ^{18}F-FBPA PET showed variable uptake in lung cancers and mediastinal tumors, benign lesions showed significantly lower SUV_{max} than those in malignant lesions ($P < 0.01$).

Conclusions: Uptake on ^{18}F-FBPA PET reflected the expression level of LAT1 in lung and mediastinal tumors. It was suggested that ^{18}F-FBPA PET can be used for the precise characterization of the tumor in pretreatment evaluation.

Key Words: LAT1, ^{18}F-FBPA, PET, lung cancer, mediastinal tumor

(*Clin Nucl Med* 2023;48: 853–860)

^{18}F-fluoro-borono-phenylalanine (^{18}F-FBPA) PET has been used for the pretreatment evaluation of boron neutron capture therapy (BNCT).[1,2] In BNCT, borono-phenylalanine (BPA) is infused, and an epithermal neutron beam is irradiated to induce a nuclear reaction to emit alpha-rays and recoil the nucleus of Li. ^{18}F-FBPA PET has been used to select candidates for BNCT and estimate the boron concentration in cancer lesions.[2,3] Recently, ^{18}F-FBPA has been proven to serve as a selective PET probe for L-type amino acid transporter-1 (LAT1).[4] LAT1 is a tumor-specific amino acid transporter that is expressed in various types of tumors, with minimal expression in normal organs.[5] L-type amino acid transporter has several subtypes. LAT2 is widely expressed in normal tissues throughout the body, whereas LAT1 is expressed in various cancers.[6] LAT1 expression is related to patient survival and can serve as an independent prognostic marker.[7]

Previous studies have reported that ^{18}F-FBPA PET can be used for tumor-specific imaging without significant uptake in inflammatory lesions, such as sarcoidosis or radiation necrosis.[8–10] However, no systematic clinical study has directly compared ^{18}F-FBPA uptake on PET with LAT1 expression in tumor lesions. Recently, LAT1 has attracted attention as a therapeutic target, and LAT1 inhibitors have been used as antitumor drugs to suppress protein synthesis by downregulating the mTORC1 signaling pathway and mobilizing the general amino acid control pathway in cancer cells.[5] High-affinity LAT1-specific inhibitors have been developed, and clinical trials have been conducted in patients with advanced solid tumors.[11] In addition, LAT1 is a novel target for radioligand therapy using amino acid analogs such as ^{131}I- or ^{211}At-labeled phenylalanine and ^{211}At-alpha-methyl-L-tyrosine.[12,13] Because the physiological expression of LAT1 is minimal in normal organs, LAT1-targeted therapy is a promising approach that can minimize adverse effects. Therefore, ^{18}F-FBPA PET is also expected to serve as an imaging modality for companion diagnostics.

In this study, we aimed to investigate LAT1 expression in preoperative patients with lung cancers or mediastinal tumors using

Received for publication April 13, 2023; revision accepted July 4, 2023.

From the *Department of Nuclear Medicine and Tracer Kinetics, †Institute for Radiation Sciences, and ‡Department of General Thoracic Surgery, Graduate School of Medicine, Osaka University; Departments of §Pharmacy, and ||Radiology, Osaka University Hospital; and Departments of ¶Molecular Imaging in Medicine, and **Bio-system Pharmacology, Graduate School of Medicine, Osaka University, Osaka, Japan.

Author contribution: T.W. and N.O. contributed to the conceptualization; T.W., N.O., S.N., E.F., T.K., T.K., S.F., H.S., T.K., K.K., K.I., M.T., and R.O. contributed to the data collection; T.W. contributed to the original draft preparation; S.N., T.K. and R.O. contributed to the review and editing; E.S., H.K., Y.K., and Y.S. contributed to the supervision. All authors have read and agreed to the submitted version of the manuscript.

Ethics approval: The study protocol was approved by the Institutional Review Board of Osaka University Hospital (approval number: 18458-5), and the study was performed in accordance with the ethical standards laid, down in the 1964 Declaration of Helsinki. Written informed consent was obtained from all patients before their inclusion in the study.

Conflicts of interest and sources of funding: The authors declare no potential conflicts of interest relevant to this study. This study was funded by the QiSS program of OPERA (grant number: JPMJOP1721) from the Japan Science and Technology Agency.

Correspondence to: Tadashi Watabe, MD, PhD, Department of Nuclear Medicine and Tracer Kinetics, Graduate School of Medicine, Osaka University, 2-2 Yamadaoka, Suita, Osaka 565-0871, Japan. E-mail: watabe.tadashi.med@osaka-u.ac.jp.

ISSN: 0363-9762/23/4810–0853
DOI: 10.1097/RLU.0000000000004816

^{18}F-FBPA PET by comparing it with immunofluorescence staining of LAT1 to validate ^{18}F-FBPA PET as a diagnostic imaging tool to estimate LAT1 expression.

PATIENTS AND METHODS

Patients

The study population comprised patients diagnosed with or suspected of having malignant tumors in the lung or mediastinal regions (n = 55 [35 males and 20 females], 15–83 [median 69] years old). The study population included patients with primary lung cancer (n = 21: adenocarcinoma [n = 13], squamous cell carcinoma [n = 5], neuroendocrine carcinoma/adenocarcinoma mixed [n = 2], and large cell carcinoma [n = 1]), lung metastases (n = 6: pharyngeal cancer [n = 2], rectal cancer [n = 2], breast cancer [n = 1], and bladder neuroendocrine carcinoma [n = 1]), thymoma (n = 10: type AB [n = 2], B1 [n = 2], B2 [n = 3], B3 [n = 2], and atypical A [n = 1]), thymic cancer (n = 2), carcinoid (n = 2), mesothelioma (n = 1), and benign tumors or lesions (n = 13). Histological diagnosis of benign tumors and lesions were cholesterol granuloma, epithelioid granuloma, mature teratoma, myelolipoma, sclerosing pneumocytoma, solitary fibrous tumor, spindle cell neoplasm, intrathymic lymphadenopathy, thymic hyperplasia, inflammation, sarcoidosis, mesothelial cyst, and thymic cyst (each n = 1). Histopathological confirmation was obtained from the surgical specimen or biopsy for all patients. Among them, 52 patients (95%) underwent surgery within 1 week after ^{18}F-FBPA PET, 1 patient underwent chemoradiation therapy before surgery (this patient was excluded from the correlation analysis with LAT1 expression in histology), and 2 patients (4%) were diagnosed with biopsy.

The study protocol was approved by the Institutional Review Board of Osaka University Hospital (approval number: 18458-5), and the study was performed in accordance with the ethical standards of the 1964 Declaration of Helsinki. Written informed consent was obtained from all patients before their inclusion in the study.

Synthesis of ^{18}F-FBPA Solution

The ^{18}F-FBPA solution was synthesized using a CFN-MPS200 (Sumitomo Heavy Industries, Tokyo, Japan) based on a previous study.[14] In brief, ^{18}F-CH_3COOF, obtained by passing ^{18}F-F_2 gas through a sodium acetate column, was reacted with 4-borono-L-phenylalanine dissolved in trifluoroacetic acid for the synthesis of ^{18}F-FBPA. After ^{18}F-FBPA was separated and purified by high-performance liquid chromatography and evaporation, it was dissolved in normal saline and then collected through a sterile 0.22 μm vented millex-GS filter into a sterile vial. The radioactivity and molar activity of the resulting ^{18}F-FBPA solution were 3265 ± 739 MBq and 236 ± 32 GBq/mmol, and its radiochemical purity was ≥98%.

PET Scanning Protocol

We used the Discovery 710 system (GE, Milwaukee, WI), which contains a cerium-doped lutetium-based scintillation crystal (LYSO, $Lu_{1.8}Y_{.2}SiO_5$:Ce) and a 64-slice CT scanner. PET scanning was performed 60 minutes after IV injection of the ^{18}F-FBPA solution (232 ± 32 MBq). PET images were acquired in 3D mode

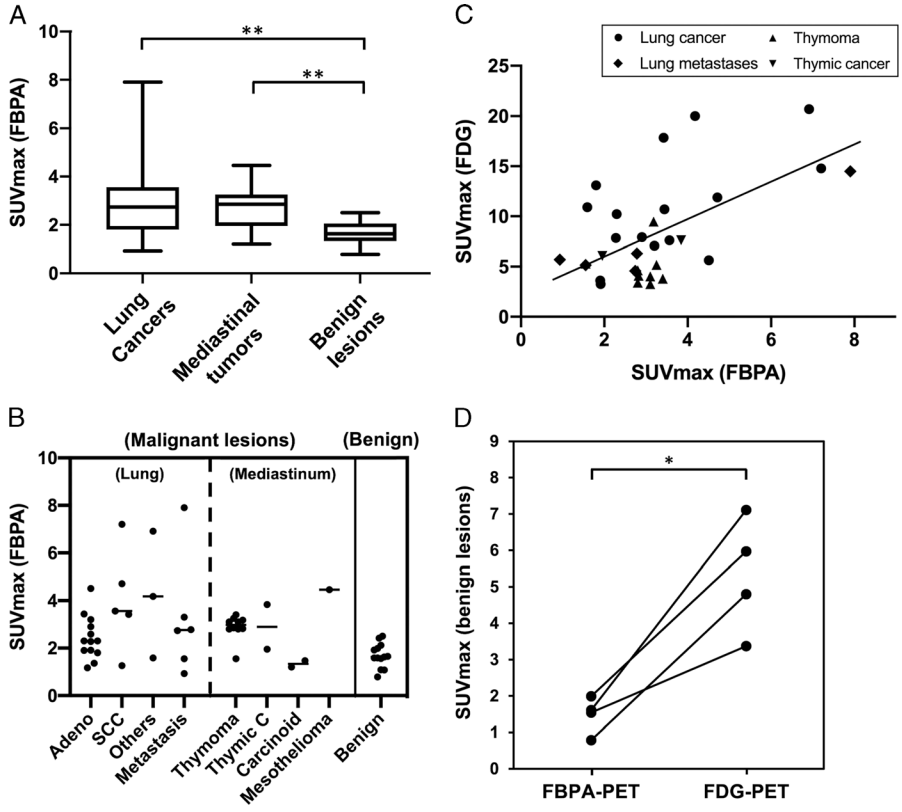

FIGURE 1. **A**, Comparison of the uptake on ^{18}F-FBPA PET among lung cancers, mediastinal tumors, and benign lesions (**$P < 0.01$ by the Dunnett test). **B**, Uptake on ^{18}F-FBPA PET (adeno, adenocarcinoma; SCC, squamous cell carcinoma; and thymic C, thymic cancer). **C**, Correlation of SUV_{max} between ^{18}F-FBPA PET and ^{18}F-FDG PET in lung cancer, lung metastases, thymoma, and thymic cancers. **D**, Comparison of SUV_{max} between ^{18}F-FBPA PET and ^{18}F-FDG PET in benign lesions. ^{18}F-FBPA PET showed low uptake values in the benign lesions, even when ^{18}F-FDG PET showed high uptake values (*$P = 0.015$ by paired t test).

(matrix, 192 × 192; pixel size, 3.65 mm; slice thickness, 3.27 mm). The scan duration was 2 minutes per bed, and scanning was performed from head to foot. The PET images were reconstructed using an ordered subset expectation maximization algorithm with time of flight, 3 iterations per 8 subsets, and Gauss filtered to a transaxial resolution of 4 mm at full width at half maximum. Attenuation correction and scatter correction were performed using the unenhanced low-dose CT data (tube voltage, 120kVp; tube current, 100 mA). The CT images were reconstructed to a slice thickness of 3.75 mm with an increment of 3.27 mm. ^{18}F-FDG PET scanning was performed 60 minutes after the IV injection of ^{18}F-FDG (3.7 MBq/kg) according to the institutional protocol. ^{18}F-FDG PET images obtained using different PET scanners were also included.

Image Analysis

The SUV measurements were performed by volume of interest analysis of the ^{18}F-FBPA PET images using Osirix MD software (Pixmeo SARL, Bernex, Switzerland). Lesion contouring was manually performed by a board-certified nuclear medicine specialist. The SUV_{max} was compared between malignant lesions (n = 27 in the lungs and n = 15 in the mediastinum) and benign lesions (n = 13). The SUV_{max} of ^{18}F-FBPA PET was compared with the immunofluorescence staining grade of LAT1.

The correlation between the SUV_{max} of ^{18}F-FBPA PET and that of ^{18}F-FDG PET (within 3 months) was compared for the available cases of malignant lesions in the lung (n = 21), thymic tumors (n = 11), and benign lesions (n = 4). The median interval between ^{18}F-FBPA PET and ^{18}F-FDG PET was 37.3 days (range, 6–95 days).

Immunofluorescence Staining of LAT1

Immunofluorescence staining was performed on resected tumor sections using an LAT1 antibody (n = 50). After deparaffinization and antigen retrieval using Liberate Antibody Binding Solution (24310, Polysciences Inc, Warrington, PA), the samples were blocked with 1% bovine serum albumin and 0.3% Triton in phosphate-buffered saline at room temperature for 30 minutes. The samples were then incubated with anti-LAT1 C-terminal antibody (rabbit polyclonal and antigen affinity purified) overnight at 4°C (1:100 dilution).[15] Fluorescence staining was performed using Alexa Fluor 568 goat anti–rabbit IgG (H + L) (A11011; Life Technologies, Thermo Fisher Scientific, Tokyo, Japan) (1:500 dilution) and DAPI Solution (340-07971; Dojindo, Kumamoto, Japan) (1:500 dilution) for 1 hour at room temperature. Staining without the primary antibody was also performed as a negative control to confirm its specificity. The stained sections were analyzed using a BZ-9000 microscope (Keyence, Osaka, Japan). LAT1 staining was graded on a 4-point scale with the consensus of 2 experts: high expression (grade 3), moderate expression (grade 2), mild expression (grade 1), and no significant expression (grade 0). Grade 3 was defined as a distinct and strong signal of LAT1 on the cell membrane in more than 70% of the tumor cells (Fig. 2B). Grade 2, 1, and 0 were defined as signal intensity of approximately 40%–70%, 10%–40%, 0%–10% on the cell membrane compared with those in the group of a grade 3 signal, respectively. The score evaluation was performed by considering the nonspecific staining with reference to the negative control section.

Statistical Analyses

Comparisons between 2 groups were performed using the paired *t* test for paired data, and comparisons among 4 groups were performed using the multiple comparison test followed by Dunnett test. The correlations between the 2 modalities were evaluated using Spearman correlation analysis. The analyses were performed using SPSS software (version 25.0, IBM Corp, Armonk, NY). Finally, *P* values <0.05 indicated statistical significance.

RESULTS

No adverse events were observed after administration of the ^{18}F-FBPA solution. Although ^{18}F-FBPA PET showed variable uptake in lung cancers (both primary and metastatic tumors) and mediastinal tumors, benign lesions indicated a significantly lower SUV_{max} value than those in malignant lesions ($P = 0.002$ and $P = 0.002$, respectively) (Fig. 1A). In mediastinal tumors, moderate uptake was observed in thymomas, thymic cancers, and mesotheliomas, whereas low uptake was observed in carcinoids (Fig. 1B). In benign lesions, ^{18}F-FBPA PET showed a low uptake (n = 13; SUV_{max}, 1.69 ± 0.51; range, 0.79–2.42).

When comparing the SUV_{max} between ^{18}F-FBPA PET and ^{18}F-FDG PET, a positive correlation was observed in lung cancer, lung metastases, thymoma, and thymic cancer (Spearman rank correlation coefficient, 0.438; $P = 0.012$) (Fig. 1C). In benign lesions,

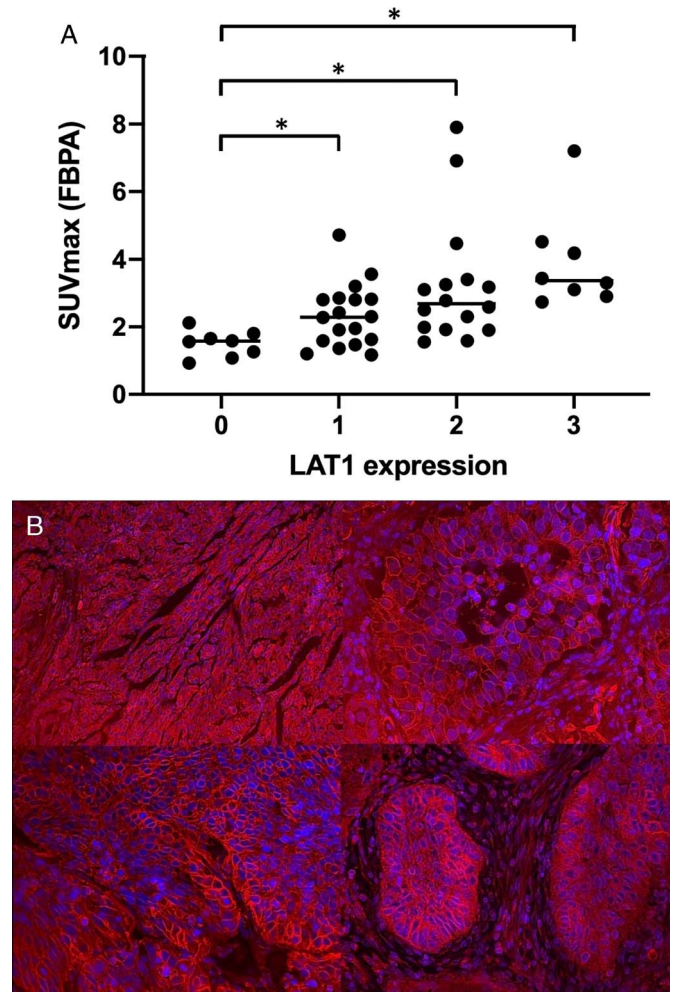

FIGURE 2. **A**, Correlation between SUV_{max} on ^{18}F-FBPA PET and LAT1 expression level by immunofluorescence staining: high expression (grade 3), moderate expression (grade 2), mild expression (grade 1), and no significant expression (grade 0) (*$P < 0.05$ by the Dunnett test). **B**, Representative immunofluorescence staining sections with high expression of LAT1 (grade 3). LAT1 is a membrane transporter and is expressed along the plasma membrane (stained in red). The nucleus is stained blue with DAPI.

TABLE 1. Patient Characteristics Including the SUV_{max} of ^{18}F-FBPA PET and ^{18}F-FDG PET, and Expression Level of LAT1 in Malignant Lesions

No.	Sex	Age	Final Diagnosis on Histology	SUV_{max} on ^{18}F-FBPA PET	SUV_{max} on ^{18}F-FDG PET	LAT1 Expression
1	M	58	Carcinoid (atypical)	1.5	(4.1)	1
2	F	60	Carcinoid (typical)	1.2	3.8	1
3	M	72	Lung cancer (adenocarcinoma)	1.8	13.1	0
4	F	45	Lung cancer (adenocarcinoma)	1.2	NA	1
5	M	75	Lung cancer (adenocarcinoma)	1.4	(1.3)	1
6	F	77	Lung cancer (adenocarcinoma)	1.9	3.3	1
7	M	80	Lung cancer (adenocarcinoma)	2.3	7.8	1
8	F	68	Lung cancer (adenocarcinoma)	2.3	NA	1
9	M	72	Lung cancer (adenocarcinoma)	3.2	7.1	1
10	F	51	Lung cancer (adenocarcinoma)	1.9	3.6	2
11	M	57	Lung cancer (adenocarcinoma)	2.3	10.2	2
12	M	56	Lung cancer (adenocarcinoma)	2.6	(26.0)	2
13	M	52	Lung cancer (adenocarcinoma)	2.9	7.9	3
14	F	47	Lung cancer (adenocarcinoma)	3.4	10.7	3
15	F	64	Lung cancer (adenocarcinoma)	4.5	5.6	3
16	M	81	Lung cancer (neuroendocrine cancer/adenocarcinoma mix)	4.2	20.0	3
17	M	75	Lung cancer (neuroendocrine cancer/adenocarcinoma mix)	1.6	10.9	2
18	F	75	Lung cancer (large cell carcinoma)	6.9	20.7	2
19	F	55	Lung cancer (squamous cell carcinoma)	1.3	1.5	0
20	M	76	Lung cancer (squamous cell carcinoma)	4.7	11.9	1
21	M	71	Lung cancer (squamous cell carcinoma)	7.2	14.8	3
22	F	71	Lung cancer (squamous cell carcinoma)	3.4	17.8	NA
23	M	78	Lung cancer (squamous cell carcinoma)	3.6	7.6	1
24	F	76	Lung metastasis (bladder neuroendocrine carcinoma)	2.8	6.3	2
25	F	66	Lung metastasis (breast cancer)	7.9	14.5	2
26	M	65	Lung metastasis (pharyngeal cancer)	2.7	4.6	3
27	M	70	Lung metastasis (pharyngeal cancer)	3.3	(6.7)	3
28	M	59	Lung metastasis (rectal cancer)	0.9	5.7	0
29	M	77	Lung metastasis (rectal cancer)	1.6	5.2	2
30	M	70	Mesothelioma	4.5	3.9	2
31	M	85	Thymic cancer	2.0	6.1	1
32	M	55	Thymic cancer	3.8	7.6	NA
33	M	57	Thymoma (atypical type A)	3.2	9.5	2
34	F	35	Thymoma (type AB)	2.8	3.4	1
35	M	75	Thymoma (type AB)	2.8	4.6	1
36	M	70	Thymoma (type B1)	3.3	5.2	2
37	F	64	Thymoma (type B1)	3.4	3.8	2
38	F	67	Thymoma (type B2)	2.8	4.1	1
39	F	73	Thymoma (type B2)	2.9	NA	1
40	M	71	Thymoma (type B2)	3.1	3.3	2
41	M	73	Thymoma (type B3)	1.6	5.3	NA
42	M	52	Thymoma (type B3)	3.1	4.0	3

The SUV_{max} of ^{18}F-FDG PET with intervals of >3 months is indicated with parenthesis.
NA, not available.

^{18}F-FBPA PET showed low uptake (SUV_{max}, 1.48 ± 0.50), even when ^{18}F-FDG PET showed high uptake (SUV_{max}, 5.31 ± 1.60) (Fig. 1D).

In the comparison between ^{18}F-FBPA uptake and LAT1 expression, a positive correlation was observed between SUV_{max} and LAT1 expression by immunofluorescence staining (Spearman rank correlation coefficient, 0.611; $P < 0.001$) (Fig. 2A). The SUV_{max} of ^{18}F-FBPA in lesions with LAT1 expression grade 3, 2, 1, and 0 were 3.92 ± 1.46, 3.21 ± 1.82, 2.33 ± 0.93, and 1.50 ± 0.39, respectively. A significant difference in SUV_{max} was observed between the LAT1 expression group (grades 1, 2, and 3) and the no expression group (grade 0). Detailed information for each patient is provided in Table 1 and Table 2. Representative immunofluorescence staining sections with high LAT1 expression (grade 3) showed high intensity in the plasma membrane (Fig. 2B).

Case presentations of ^{18}F-FBPA PET and immunofluorescence images of LAT1 staining are shown in Figures 3 to 5. The uptake of ^{18}F-FBPA PET corresponded to the histological expression level of LAT1 (Figs. 3–5). PET images of a patient with reactive

TABLE 2. Patient Characteristics Including the SUV_{max} of ^{18}F-FBPA PET and ^{18}F-FDG PET, and Expression Level of LAT1 in Benign Lesions

No.	Sex	Age	Final Diagnosis on Histology	SUV_{max} on ^{18}F-FBPA PET	SUV_{max} on ^{18}F-FDG PET	LAT1 Expression
1	F	61	Cholesterol granuloma	2.0	6.0	2
2	F	70	Epithelioid granuloma	1.6	NA	1
3	M	74	Inflammation	0.8	4.8	NA
4	M	79	Intrathymic lymphadenopathy	1.6	7.1	0
5	F	30	Mature teratoma	1.7	NA	0
6	M	71	Mesothelial cyst	1.1	NA	0
7	M	64	Myelolipoma	1.6	NA	1
8	M	62	Sarcoidosis	1.9	NA	2
9	M	18	Sclerosing pneumocytoma	2.5	NA	2
10	M	33	Solitary fibrous tumor	2.1	NA	0
11	F	15	Spindle cell neoplasm	2.4	(5.9)	1
12	M	67	Thymic cyst	1.1	(3.4)	NA
13	M	71	Thymic hyperplasia	1.6	3.4	0

The SUV_{max} of ^{18}F-FDG PET with intervals of >3 months is indicated with parenthesis.
NA, not available.

lymph nodes (benign lesion) with high uptake of ^{18}F-FDG and low uptake of ^{18}F-FBPA are shown in Figure 6.

DISCUSSION

In this study, we evaluated patients with lung cancer (primary tumor and lung metastases), mediastinal tumors, and benign lesions using ^{18}F-FBPA PET with immunohistological comparison. A moderate correlation was observed between ^{18}F-FBPA uptake and histological LAT1 expression levels. It was suggested that ^{18}F-FBPA PET can be used for the precise characterization of the tumor in pretreatment evaluation. It was also expected to serve as imaging for companion diagnostics for the LAT1-targeted therapy, such as antitumor therapy using an LAT1 inhibitor and radioligand therapy targeting LAT1.[12,13,16] Nanvuranlat (JPH203), a novel selective LAT1 inhibitor, has been investigated in advanced refractory biliary tract cancer in a phase II clinical trial and demonstrated a statistically significant improvement in progression-free survival in comparison with the placebo group (clinical trial registration number: UMIN000034080).[17] Therefore, appropriate diagnostic imaging for the evaluation of LAT1 is required for its expansion to other cancer types.

As shown in this study, variable degrees of expression were observed in malignant tumors; therefore, LAT1 expression should be evaluated by ^{18}F-FBPA PET in each patient. Previous studies have reported the LAT1 expression rate to be 91% (91/100) in lung squamous cell carcinoma,[18] 29% (58/200) in lung adenocarcinoma,[18] 61% (50/84) in hepatocellular carcinoma,[19] 64% (71/110) in pancreatic ductal adenocarcinoma,[20] and 43% (56/129) in colon cancer.[21] The higher expression rate of LAT1 in squamous cell carcinoma than in adenocarcinoma corresponds to our ^{18}F-FBPA PET results (Fig. 1B).

In the immunofluorescence staining of LAT1, lesions without LAT1 expression (grade 0) showed significantly lower SUV_{max} than those with LAT1 expression (grade 1–3). Our previous study indicated that ^{18}F-FBPA is a specific substrate for LAT1.[4] ^{18}F-FBPA PET can be superior to immunofluorescence staining as it can evaluate the whole tumor lesion in 3D compared with a 1D slice histological evaluation, which may not capture the heterogeneity of LAT1 tumor expression. Therefore, ^{18}F-FBPA PET could be used to exclude patients with lesions without LAT1 expression, which is not suitable for LAT1-targeted therapy. Furthermore, the optimal SUV_{max} threshold for ^{18}F-FBPA PET could be determined to obtain a therapeutic effect using companion diagnostic imaging for appropriate patient selection.

^{18}F-FDG PET is now routinely used for the characterization of tumor lesions and staging before therapy or surgery. However, some benign tumors or inflammatory lesions show high ^{18}F-FDG uptake, hindering the differentiation between malignant and nonmalignant lesions.[22,23] Recently, fibroblast activation protein inhibitor PET has attracted attention as a pantumor probe because of its higher sensitivity than ^{18}F-FDG PET.[24] However, benign uptake of fibroblast activation protein inhibitor can be higher than that of ^{18}F-FDG, such as during pancreatitis or posttreatment changes.[25] Compared with ^{18}F-FDG PET, ^{18}F-FBPA PET showed low physiological uptake in normal organs except for urine excretion, indicating a higher diagnostic efficacy and avoiding false-positive findings.[2] Therefore, tumor-specific imaging using ^{18}F-FBPA PET can be used to precisely characterize tumor lesions or detect true metastatic lesions.

Isohashi et al[10] compared ^{18}F-FBPA PET and ^{18}F-FDG PET in various types of malignant tumors or benign lesions, and reported that the SUV_{max} of ^{18}F-FBPA PET was significantly higher for malignant tumors than for benign lesions (5.1 ± 3.0 vs 2.9 ± 0.6, $P < 0.01$). The best SUV_{max} cutoff of ^{18}F-FBPA for distinguishing malignant tumors from benign lesions was 3.24 for ^{18}F-FBPA PET (sensitivity, 0.818; specificity, 0.753). In our study, the highest SUV_{max} of benign lesions was 2.5 for ^{18}F-FBPA PET, and the lowest cutoff value might be more appropriate for our cohort as the SUV_{max} of lung adenocarcinoma ranged from 1.2 to 4.5 on ^{18}F-FBPA PET. Igaki et al[26] reported that the SUV_{max} of ^{18}F-FBPA PET correlated well with that of ^{18}F-FDG PET (Pearson correlation coefficient, 0.74).[27] In our study, we observed a positive correlation between ^{18}F-FBPA PET and ^{18}F-FDG PET in the lung and thymic malignancies, which was consistent with their report. However, we should be careful about false-positive findings owing to high ^{18}F-FDG-uptake in benign lesions as shown in Figure 1D. Tatsumi et al[28] reported that ^{18}F-FBPA PET can detect the early response to anti–PD-1 immunotherapy in melanoma-bearing mice, whereas ^{18}F-FDG PET could not detect this response.[29] ^{18}F-FBPA PET is suggested to serve as a sensitive modality for evaluating treatment efficacy in the early phase of anti–PD-1 immunotherapy. Based on the above reports, ^{18}F-FBPA PET is highly useful for

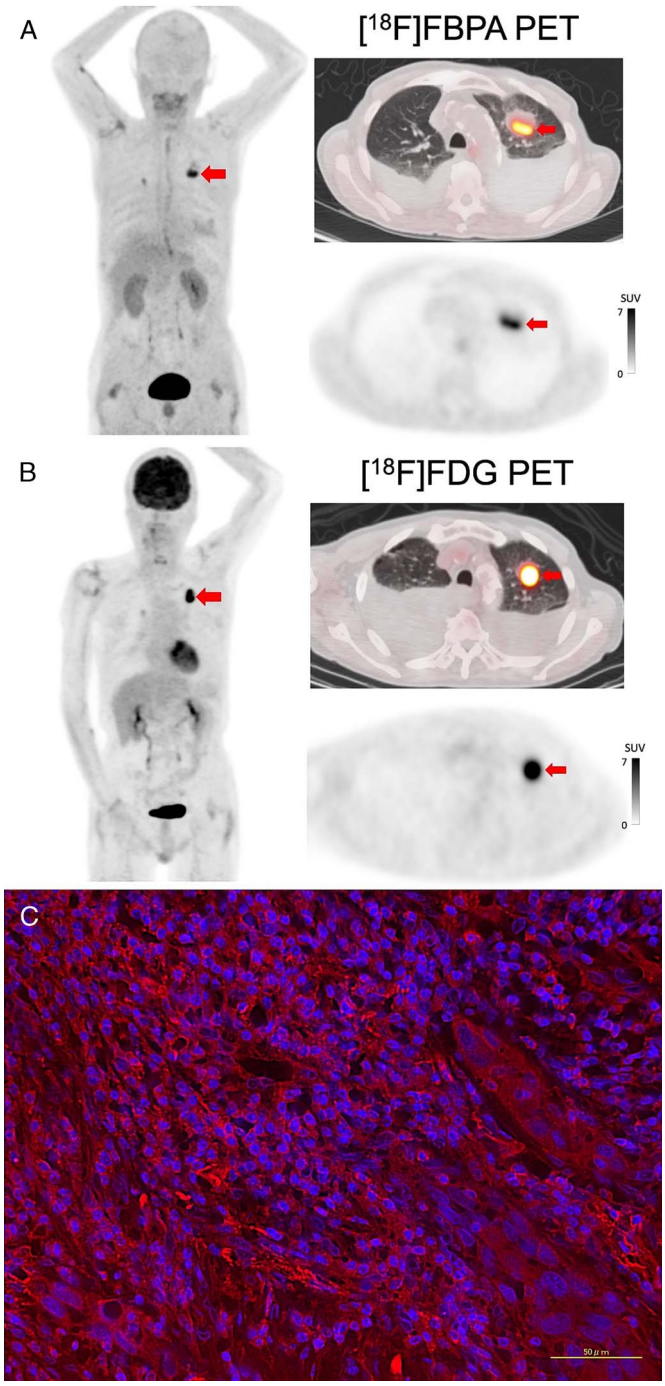

FIGURE 3. A 71-year-old man with primary lung cancer (squamous cell carcinoma): (**A**) ^{18}F-FBPA PET and (**B**) ^{18}F-FDG PET: MIP and axial PET/CT fusion and PET images (arrows indicate the primary lesion; SUV_{max} of 7.2 on ^{18}F-FBPA PET and SUV_{max} of 14.8 on ^{18}F-FDG PET). **C**, Immunofluorescence-staining section showing high LAT1 expression (grade 3).

distinguishing between benign and malignant lesions, and for evaluating therapeutic effects in cases where ^{18}F-FDG PET shows reactive accumulation.

Recently, there is growing interest in theranostics, which integrates therapeutics and diagnostics. LAT1-targeted imaging and therapy is a promising approach, because LAT1 is a tumor-specific transporter with minimal expression in normal organs. Therefore, the future expansion of clinical applications is

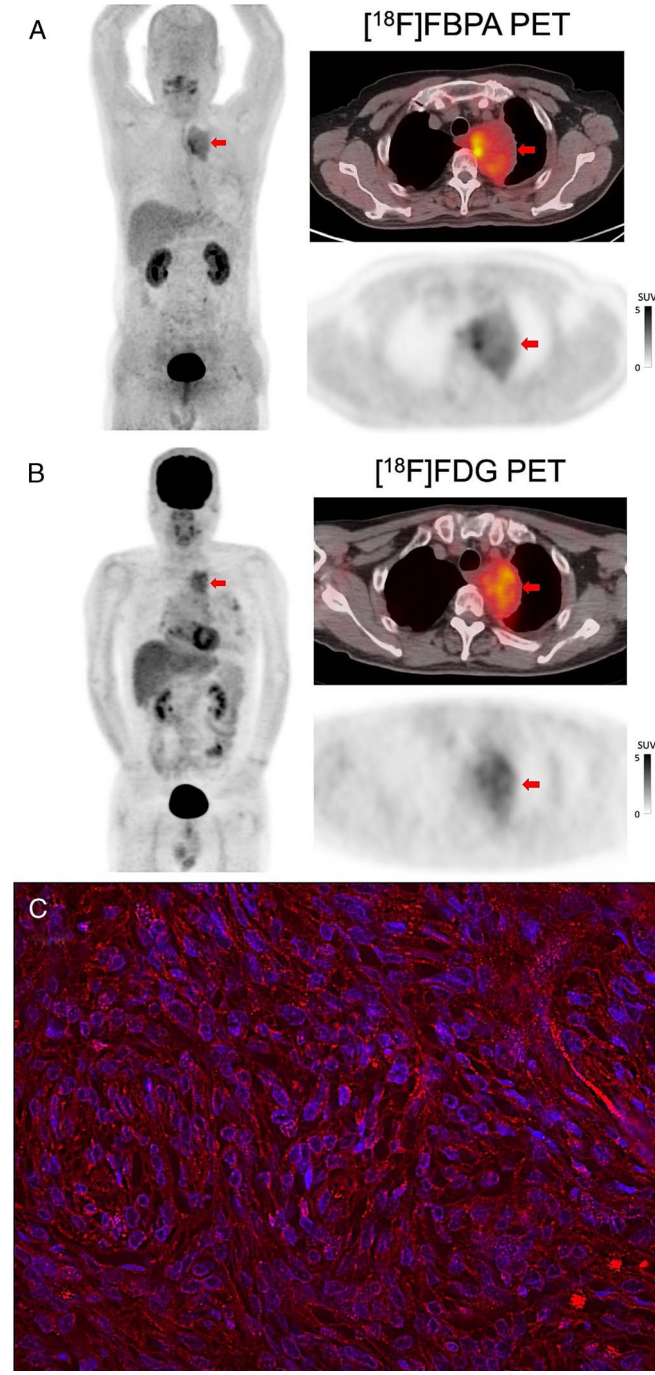

FIGURE 4. A 70-year-old man with mesothelioma: (**A**) ^{18}F-FBPA PET and (**B**) ^{18}F-FDG PET: MIP and axial PET/CT fusion and PET images (arrows indicate primary lesion; SUV_{max} of 4.46 on ^{18}F-FBPA PET and SUV_{max} of 3.92 on ^{18}F-FDG PET). **C**, Immunofluorescence-staining section showing moderate LAT1 expression (grade 2).

expected for selective LAT1 inhibitors or LAT1-radioligand therapy. ^{18}F-FBPA PET could serve as a companion diagnostic imaging to select appropriate patients for such therapy.

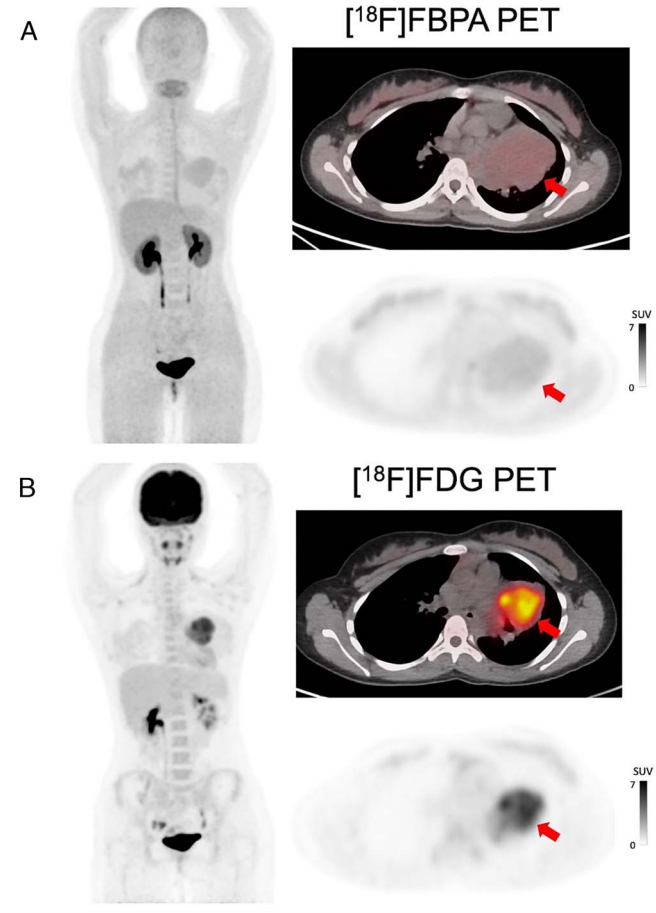

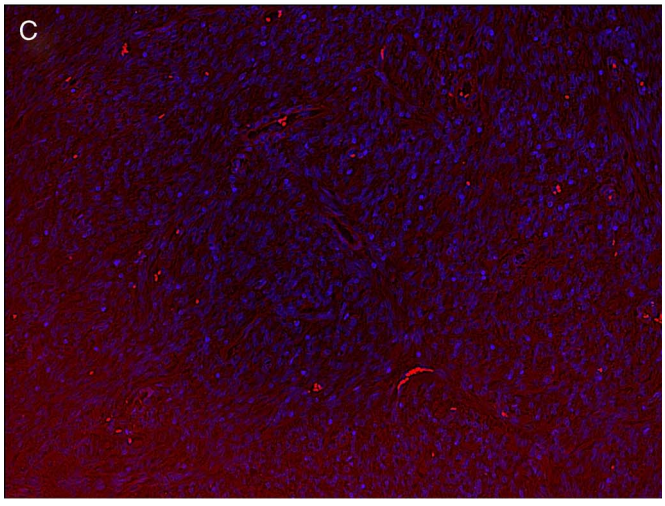

FIGURE 5. A 15-year-old girl with a spindle cell tumor (benign tumor): (**A**) ^{18}F-FBPA PET and (**B**) ^{18}F-FDG PET: MIP and axial PET/CT fusion and PET images (arrows indicate the tumor lesion; SUV_{max} of 2.4 on ^{18}F-FBPA PET and SUV_{max} of 5.9 on ^{18}F-FDG PET). **C**, Immunofluorescence-staining section showing low LAT1 expression (grade 1).

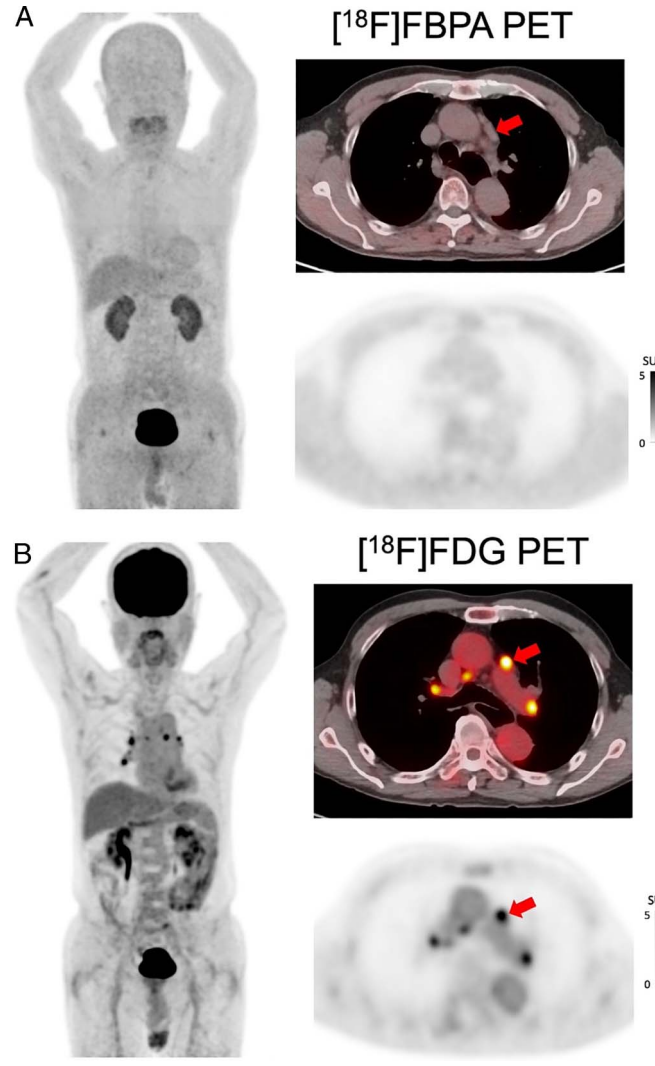

FIGURE 6. A 79-year-old man with reactive lymph nodes: (**A**) ^{18}F-FBPA PET and (**B**) ^{18}F-FDG PET: MIP and axial PET/CT fusion and PET images (arrows indicate the reactive lymph nodes; SUV_{max} of 1.6 on ^{18}F-FBPA PET and SUV_{max} of 7.1 on ^{18}F-FDG PET).

This study had some limitations. First, the number of patients with each tumor subtype was small. Second, we performed ^{18}F-FBPA PET after ^{18}F-FDG PET with a median of 37 days' intervals, and some ^{18}F-FDG PET images were acquired using different PET scanners, which may have resulted in a biased comparison. Third, we included patients specifically with chest lesions, and future studies should be performed to evaluate other cancers, especially abdominal lesions, to expand the applicability of ^{18}F-FBPA PET.

CONCLUSIONS

This study showed that uptake on ^{18}F-FBPA PET reflected the expression of LAT1 in lung and mediastinal tumors. Although variable uptake was observed on ^{18}F-FBPA PET, benign lesions showed significantly lower uptake than malignant lesions. ^{18}F-FBPA PET can be used for the precise characterization of the tumor in pretreatment evaluation.

REFERENCES

1. Ishiwata K. 4-Borono-2-^{18}F-fluoro-L-phenylalanine PET for boron neutron capture therapy-oriented diagnosis: overview of a quarter century of research. *Ann Nucl Med*. 2019;33:223–236.
2. Shimosegawa E, Isohashi K, Naka S, et al. Assessment of ^{10}B concentration in boron neutron capture therapy: potential of image-guided therapy using ^{18}FBPA PET. *Ann Nucl Med*. 2016;30:749–755.
3. Hanaoka K, Watabe T, Naka S, et al. FBPA PET in boron neutron capture therapy for cancer: prediction of (10)B concentration in the tumor and normal tissue in a rat xenograft model. *EJNMMI Res*. 2014;4:70.
4. Watabe T, Ikeda H, Nagamori S, et al. ^{18}F-FBPA as a tumor-specific probe of L-type amino acid transporter 1 (LAT1): a comparison study with ^{18}F-FDG and ^{11}C-methionine PET. *Eur J Nucl Med Mol Imaging*. 2017;44:321–331.
5. Kanai Y. Amino acid transporter LAT1 (SLC7A5) as a molecular target for cancer diagnosis and therapeutics. *Pharmacol Ther*. 2022;230:107964.
6. Kaira K, Oriuchi N, Imai H, et al. l-type amino acid transporter 1 and CD98 expression in primary and metastatic sites of human neoplasms. *Cancer Sci*. 2008;99:2380–2386.
7. Kaira K, Sunose Y, Arakawa K, et al. Prognostic significance of L-type amino-acid transporter 1 expression in surgically resected pancreatic cancer. *Br J Cancer*. 2012;107:632–638.
8. Beshr R, Isohashi K, Watabe T, et al. Preliminary feasibility study on differential diagnosis between radiation-induced cerebral necrosis and recurrent brain tumor by means of [^{18}F]fluoro-borono-phenylalanine PET/CT. *Ann Nucl Med*. 2018;32:702–708.
9. Watabe T, Shimamoto H, Naka S, et al. ^{18}F-FBPA PET in sarcoidosis: comparison to inflammation-related uptake on FDG PET. *Clin Nucl Med*. 2020;45:863–864.
10. Isohashi K, Kanai Y, Aihara T, et al. Exploration of the threshold SUV for diagnosis of malignancy using ^{18}F-FBPA PET/CT. *Eur J Hybrid Imaging*. 2022;6:35.
11. Okano N, Naruge D, Kawai K, et al. First-in-human phase I study of JPH203, an L-type amino acid transporter 1 inhibitor, in patients with advanced solid tumors. *Invest New Drugs*. 2020;38:1495–1506.
12. Watabe T, Kaneda-Nakashima K, Shirakami Y, et al. Targeted alpha therapy using astatine (^{211}At)-labeled phenylalanine: a preclinical study in glioma bearing mice. *Oncotarget*. 2020;11:1388–1398.
13. Kaneda-Nakashima K, Zhang Z, Manabe Y, et al. α-Emitting cancer therapy using ^{211} At-AAMT targeting LAT1. *Cancer Sci*. 2021;112:1132–1140.
14. Naka S, Watanabe T, Kanai Y, et al. Improved stability and practicality for synthesis of 4-borono-2-[^{18}F]fluoro-l-phenylalanine by combination of [^{18}O]O_2 single-use and [^{18}F]CH_3COOF labeling agents. *Nucl Med Mol Imaging*. 2022;56:86–95.
15. Matsuo H, Tsukada S, Nakata T, et al. Expression of a system L neutral amino acid transporter at the blood-brain barrier. *Neuroreport*. 2000;11:3507–3511.
16. Okanishi H, Ohgaki R, Xu M, et al. Phosphoproteomics revealed cellular signals immediately responding to disruption of cancer amino acid homeostasis induced by inhibition of L-type amino acid transporter 1. *Cancer Metab*. 2022;10:18.
17. Furuse J, Ikeda M, Ueno M, et al. Nanvuranlat, an L-type amino acid transporter (LAT1) inhibitor for patients with pretreated advanced refractory biliary tract cancer (BTC): primary endpoint results of a randomized, double-blind, placebo-controlled phase 2 study. 2023 ASCO GI Cancers Symposium. *J Clin Oncol*. 2023;41:494.
18. Kaira K, Oriuchi N, Imai H, et al. Prognostic significance of L-type amino acid transporter 1 expression in resectable stage I-III nonsmall cell lung cancer. *Br J Cancer*. 2008;98:742–748.
19. Namikawa M, Kakizaki S, Kaira K, et al. Expression of amino acid transporters (LAT1, ASCT2 and xCT) as clinical significance in hepatocellular carcinoma. *Hepatol Res*. 2015;45:1014–1022.
20. Altan B, Kaira K, Watanabe A, et al. Relationship between LAT1 expression and resistance to chemotherapy in pancreatic ductal adenocarcinoma. *Cancer Chemother Pharmacol*. 2018;81:141–153.
21. Furuya M, Horiguchi J, Nakajima H, et al. Correlation of L-type amino acid transporter 1 and CD98 expression with triple negative breast cancer prognosis. *Cancer Sci*. 2012;103:382–389.
22. Higashi T, Saga T, Nakamoto Y, et al. Diagnosis of pancreatic cancer using fluorine-18 fluorodeoxyglucose positron emission tomography (FDG PET)—usefulness and limitations in "clinical reality". *Ann Nucl Med*. 2003;17:261–279.
23. Hurwitz R. F-18 FDG positron emission tomographic imaging in a case of ruptured breast implant: inflammation or recurrent tumor? *Clin Nucl Med*. 2003;28:755–756.
24. Dendl K, Koerber SA, Kratochwil C, et al. FAP and FAPI-PET/CT in malignant and non-malignant diseases: a perfect symbiosis? *Cancers (Basel)*. 2021;13:4946.
25. Pang Y, Zhao L, Shang Q, et al. Positron emission tomography and computed tomography with [^{68}Ga]Ga-fibroblast activation protein inhibitors improves tumor detection and staging in patients with pancreatic cancer. *Eur J Nucl Med Mol Imaging*. 2022;49:1322–1337.
26. Igaki H, Nakamura S, Kurihara H, et al. Comparison of ^{18}FBPA uptake with ^{18}FDG uptake in cancer patients. *Appl Radiat Isot*. 2020;157:109019.
27. Chen H, Pang Y, Li J, et al. Comparison of [^{68}Ga]Ga-FAPI and [^{18}F]FDG uptake in patients with gastric signet-ring-cell carcinoma: a multicenter retrospective study. *Eur Radiol*. 2023;33:1329–1341.
28. Tatsumi M, Soeda F, Naka S, et al. Advantages of FBPA PET in evaluating early response of anti-PD-1 immunotherapy in B16F10 melanoma-bearing mice: comparison to FDG PET. *Front Oncol*. 2022;12:1026608.
29. Hotta M, Rieger AC, Jafarvand MG, et al. Non-oncologic incidental uptake on FAPI PET/CT imaging. *Br J Radiol*. 2022;96:20220463.